

Archaeoseismological investigation of the deformation of the ruin of the crusader fortress Ateret, Israel with 3DEC

G. Schweppe^{1,2}, K.-G. Hinzen² & S. Marco³

¹Itasca Consulting GmbH, Gelsenkirchen, Germany

²Earthquake Geology and Archaeoseismology Group, Institute of Geology and Mineralogy, Cologne University, Bergisch Gladbach, Germany

³Department of Geophysics, Tel Aviv University, Tel Aviv, Israel

1 INTRODUCTION

The Crusader Fortress of Tell Ateret in Israel was built on the western bank of the Jordan about 13 km north of the Sea of Galilee on top of a ridge which is traversed by the Dead Sea Transform Fault (DSTF). The Fortress in the Jordan Valley was conquered and destroyed during construction by Muslim forces in 1179 (Marco *et al.* 1997, Ellenblum *et al.* 1998). The northern and southern fortification walls show significant lateral offset (*cf.* Fig. 1) that is related to movement along the fault line of the DSTF.

The DSTF is the main tectonic feature in the Middle East, a major tectonic plate boundary which has been active since the Miocene (about 12 Mio years) and connects, over a distance of 1000 km, the opening of the Red Sea in the south with the East Anatolian Fault System of the Bitlis-Zagros collision zone in the north (Quennell 1956, Freund *et al.* 1968). The strike slip fault has a sinistral movement characteristic and marks the boundary between the Arabian plate and Sinai subplate. GPS measurements estimated an overall short-term sinistral slip of 4-6 mm/yr (Wdowinski *et al.* 2004, Gomez *et al.* 2007, Sadeh *et al.* 2012), which matches the long-term geologic rates estimated by a 105 km offset of pre-Miocene geologic formations in Israel (Quennell 1956, Freund 1965, Bartov *et al.* 1980).

The seismicity of Israel is characterized by infrequent large earthquakes with periods of small to moderate earthquakes in between (Begin *et al.* 2005, Agnon 2014). The historical records of Israel reach back about 3000 years and give comprehensive information about pre-instrumental earthquakes of the area (Ambraseys 1971). With this wealth of information and additional interdisciplinary, independent archaeo- and palaeo-seismological research it was possible to compile earthquake catalogs for the last 2000 years (*e.g.*-Ambraseys 2009, Guidoboni *et al.* 1994, Guidoboni & Comastri 2005, Sbeinati *et al.* 2005)

After the Ateret site was abandoned in 1179 two large earthquakes occurred on the DSTF in close vicinity to the ruin. Ellenblum *et al.* 2015 concluded that the 20 May 1202 earthquake with a Magnitude (M_s) of 7.4 (Ambraseys & Melville 1988) deformed the fortification walls first and the 30 October 1759 earthquake with an M_s of 6.6 (Ambraseys & Barazangi 1989) deformed the walls a second time. The deformation observed at the ruin is assigned to the two above mentioned earthquakes, due to the good temporal correlation.

To gain more information from the deformation pattern a Discrete Element (DE) model of the northern section of the fortification wall was developed in 3DEC (Itasca 2016). Questions addressed with the model were:

- Does the dislocation velocity affect the deformation pattern of the fortification walls?
- Is it possible to decide, based on the deformation pattern of the wall, whether the total offset is the result of a rapid coseismic movement or does slow creep movement have to be considered as well?
- Can new insights be gained on the dislocation velocity of the individual events?

- Is it possible to discern the amount of slip by which the two sides of the fault contributed to the total displacement? And in the case of a coseismic displacement, a follow up question is: Is it possible to distinguish between the effects of the two earthquakes?

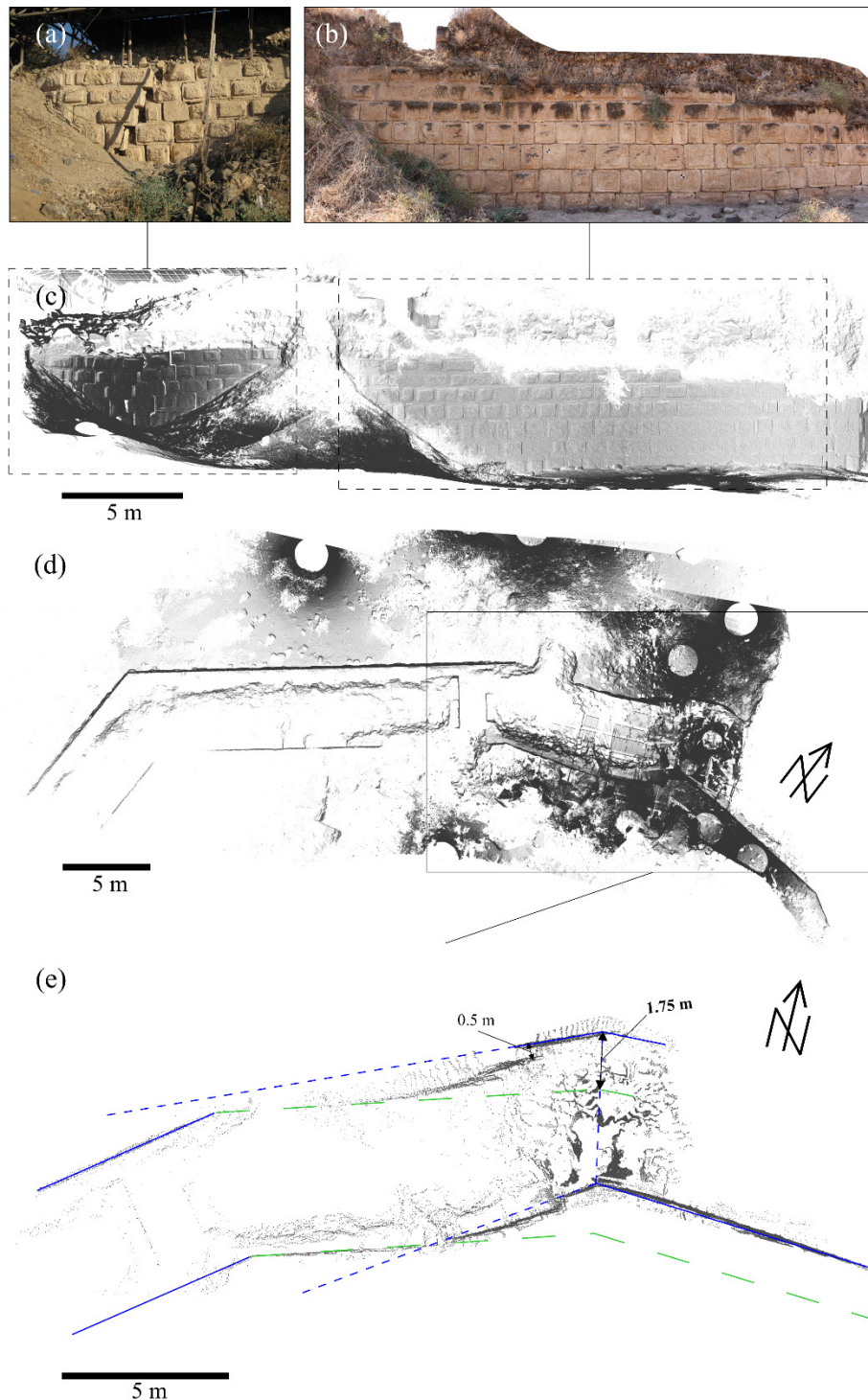


Figure 1. (a) Photo of the offset northern wall from outside of the fortress (view southward). (b) Photo of the northern wall west of the offset from outside of the fortress. (c) 3D laser scan model of the northern wall seen from the outside of the fortress. The sections covered by the photos from (a) and (b) are marked with dashed rectangles. (d) Top view of the scan model of the northern fortification wall. The section inside the rectangle is magnified in: (e) Laser scanning points are shown in grey. The blue solid lines mark the current position of the ruptured wall. Blue dashed lines are the extrapolation of the current wall position while the dashed green lines show the inferred original position.

The model building, analysis strategy, and results are briefly summarized in the following sections.

2 RECONSTRUCTION AND ANALYSIS

As a first step, the archaeological site was extensively surveyed with 3D laser scans (*cf.* Fig. 1 c-e). Based on the resulting 3D point clouds and historical information the original course of the northern fortification wall was reconstructed, which is required for the development of the DE model. Also, the survey information was vital to be able to compare the results of the simulation with the actual deformation pattern.

The fortification walls were constructed in an *opus implectum* style: two shells of massive well worked limestone ashlars. Between the two shells is a gap of 3.4 m, filled with a mixture of basalt cobbles and mortar. During construction the inner and outer shell were covered by construction ramps, as no further construction utilities, such as cranes, were used. After the fortress was conquered, large parts of the fortification walls survived the destruction, as they were covered by the ramps. Archaeological evidence shows that the fortification walls were also covered by the ramps when the damaging earthquakes occurred. The walls were partly exposed by archaeologists in the 1990s. The 3D laser scans reveal a total offset of 1.75 m (*cf.* Fig. 1e) of the northern wall.

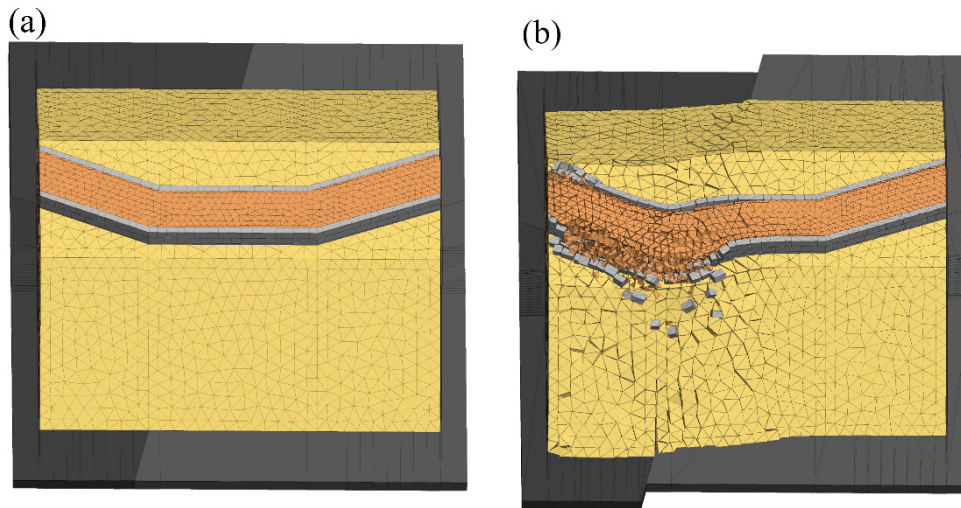


Figure 2. (a) Initial state of the model before the simulation from a northern perspective. The construction ramps are shown in a sandy yellow color. Both shells are shown in light grey and the filling between the shells in orange. The two parted baseplate representing the eastern and western plate are shown in dark and lighter dark grey, respectively. (b) example of the model state after the simulation from the same perspective and color scheme than (a).

The DE model is comprised of four main parts (*cf.* Fig. 2a): First, a two-part baseplate simulating the Sinai subplate and Arabian plate. Second, the shells of the fortification walls, where the blocks represent the well-worked ashlars. Third, the filling between the shells, and lastly, the constructions ramps, which cover the inner and outer shell. The last two parts were realized in the model by using the bonded block model (BBM) approach to enable movement in these parts. The resulting model was composed of 52,864 rigid blocks in total. The mortar was simulated by the joint properties.

In total 54 simulations, separated into two scenarios, were carried out with this *3DEC* model. The first scenario covered different movement directions of the ground-plates with different displacement velocities to investigate the influence movement direction and velocity to the deformation ranging from 0.1 to 5 m/s. The left lateral movement observed at the DSTF can be achieved by different absolute directions of both plates:

- Only the Arabian (eastern) plate moves north
- Only the Sinai (western) plate moves south
- Arabian plate moves north and the Sinai plate south
- Both plates move north where the Arabian plate moves twice the amount of the Sinai plate.

In a second scenario the goal was to represent the two earthquakes. Therefore, in a first movement the baseplate was shifted by 1.25 m with different velocities and in a second movement the already offset model was again shifted by 0.5 m with different velocities. An example of the end state of a simulation is shown in Figure 2b.

3 RESULTS AND DISCUSSION

To estimate how well the simulated deformation matches the actual deformation at the northern fortification wall, the position of the end point of the blocks must be compared with the *in situ* measured deformation. First, the best fit between both datasets was calculated by an Iterative Closest Point (ICP) algorithm. Next, the median of the residual distances between the measured and simulated points and the mean deviation (MD) of the median were used as measures of the fit.

In Figure 3 the results of the first scenario are shown. It is evident that the direction of movement and the velocity has significant influence on the deformation. The simulations where only the Arabian plate moves north show overall the best fit with the observed deformation preferably the one with a displacement velocity of 3 m/s.

Figure 4 summarizes the results of the second scenario. In these simulations, according to the results of the first scenario, only the Arabian Plate moved north. The simulation where the baseplate is first displaced by an amount of 1.25 m with a velocity of 3 m/s and then by 0.5 m with 1 m/s shows the best fit.

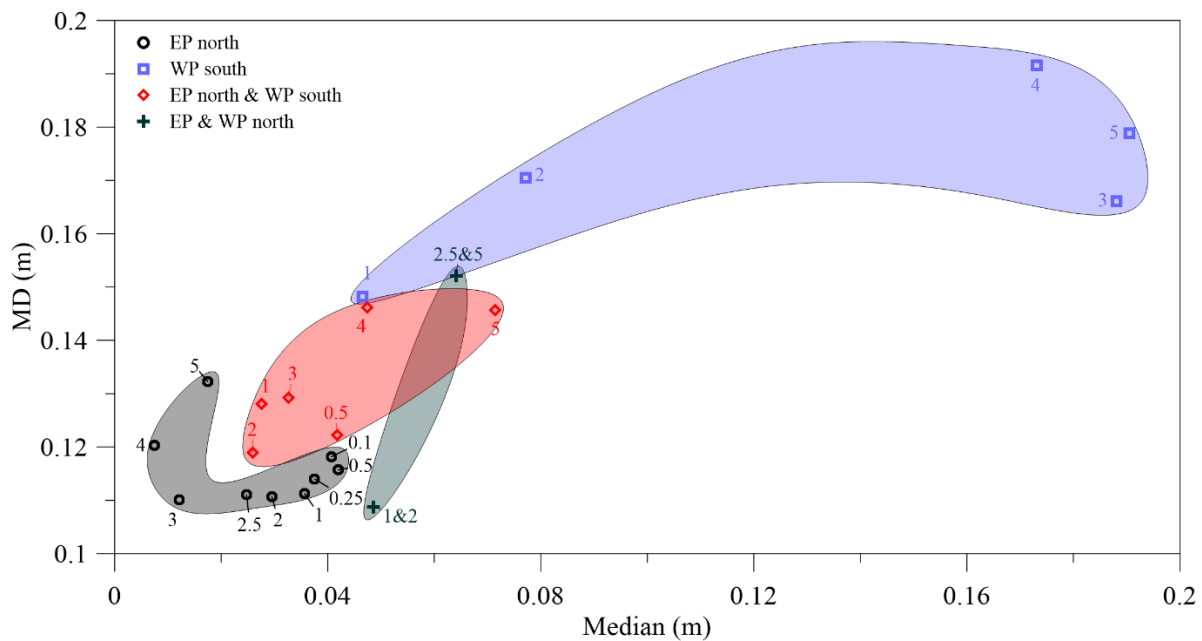


Figure 3. Mean deviation from the median (MD) plotted versus the median of the residual distances of all simulations of the first scenario. Results with the same direction of ground motion are outlined by polygonal splines with the same color. The labels show the velocity (m/s) of the according simulation; (EP = Eastern Plate and WP = Western Plate).

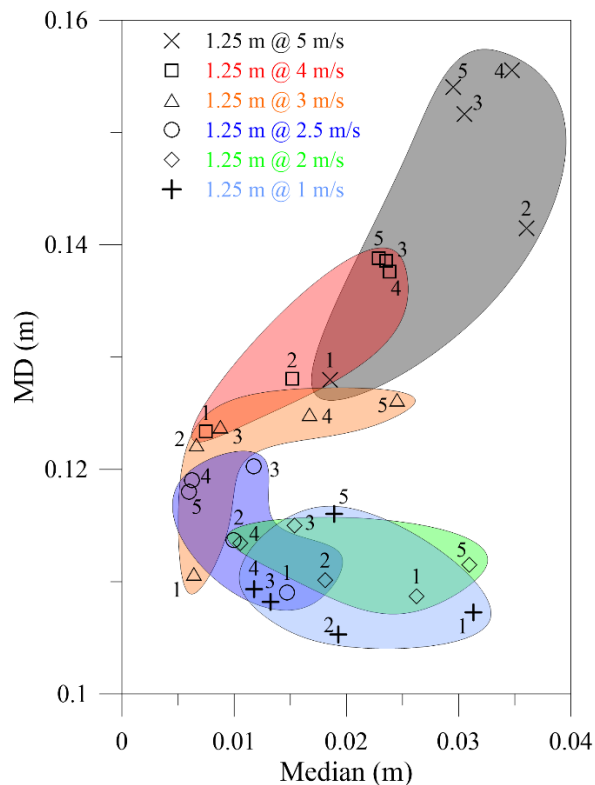


Figure 4. Mean deviation from the median (MD) plotted versus the median of the residual distance of all simulations of the second scenario. Simulations with the same first stage are highlighted with the same color. The labels show the velocity (m/s) of the according simulation.

4 CONCLUSIONS

A DE model of the northern fortification wall of the Ateret Crusader fortress, using *3DEC* with a bonded block model approach, proved able to back-calculate the deformation caused by the two earthquakes. The results of the simulation support the previous assumption that the deformation was caused by two consecutive coseismic displacements. The main movement occurred on the Arabian plate, while the Sinai subplate was locked. The slip velocities during the earthquakes on 20 May 1202 and on 30 October 1759 were estimated to be 3 m/s and 1 m/s, respectively.

REFERENCES

- Agnon, A. 2014. *Pre-Instrumental Earthquakes Along the Dead Sea Rift*, in *The Dead Sea Transform Fault System: Reviews*, Z. Garfunkel, Z. Ben-Avraham, and E. Kagan (Eds.), Springer, Dordrecht, 207-261.
- Ambraseys, N.N. 1971. Value of Historical Records of Earthquakes, *Nature* 232, 375-379.
- Ambraseys, N.N. & Melville, C.P. 1988. An Analysis of the Eastern Mediterranean Earthquake of 20 May 1202, in *Historical Seismograms and Earthquakes of the World*, W. H. K. Lee, H. Meyers, and K. Shimanzki (Eds.), Academic Press, San Diego, 181-200.
- Ambraseys, N.N. & Barazangi, M. 1989. The 1759 Earthquake in the Bekaa Valles: Implications for Earthquake Hazard Assessment in the Eastern Mediterranean Region, *J. Geophys. Res.* 94, 4007-4013.
- Ambraseys, N.N. 2009. *Earthquakes in the Mediterranean and Middle East: A Multidisciplinary Study of Seismicity up to 1900*, Cambridge University Press, Cambridge, 947 p.
- Bartov, Y., Steinitz, G., Eyal, M. & Eyal, Y. 1980. Sinistral Movement Along the Gulf of Aqaba - Its Age and Relation to the Opening of the Red Sea, *Nature* 285, 220-221.
- Ellenblum, R., Marco, S., Agnon, A., Rockwell, T. & Boas, A. 1998. Crusader Castle Torn Apart by Earthquake at Dawn, 20 May 1202, *Geology* 26, 303-306.

- Ellenblum, R., Marco, S., Kool, R., Davidovitch, U., Porat, R. & Agnon, A. 2015. Archaeological Record of Earthquake Ruptures in Tell Ateret, the Dead Sea Fault, *Tectonics* 34, 2105–2117.
- Freund, R. 1965. A Model for the Structural Development of Israel and Adjacent Areas Since Upper Cretaceous Times, *Geol. Mag.* 102, 189-205.
- Freund, R., Zak, I. & Garfunkel, Z. 1968. Age and Rate of the Sinistral Movement Along the Dead Sea Rift, *Nature* 220, 253-255.
- Gomez, F., Karam, G., Khawlie, M., McClusky, S., Vernnt, P., Reilinger, R., Jaafar, R., Tabet, C., Khair, K. & Barazangi, M. 2007. Global Positioning System Measurements of Strain Accumulation and Slip Transfer Through the Restraining Bend Along the Dead Sea Fault System in Lebanon, *Geophys. J. Int.* 168, 1021-1028.
- Guidoboni, E., Comastri, A. & Traina, G. 1994. Catalogue of Ancient Earthquakes in the Mediterranean Area up to the 10th Century, Istituto Nazionale di Geofisica, Bologna, 504 p.
- Guidoboni, E. & Comastri, A. 2005. Catalogue of Ancient Earthquakes and Tsunamis the Mediterranean Area from 11th to the 15th Century, Istituto Nazionale di Geofisica, Bologna, 1037p.
- Itasca Consulting Group, Inc. 2016. *3DEC – 3-Dimensional Distinct Element Code, Ver. 5.2*. Minneapolis: Itasca.
- Marco, S., Agnon, A., Ellenblum, R., Eidelman, A., Basson, U. & Boas, A. 1997. 817-Year-Old Walls Offset Sinistral 2.1 m by the Dead Sea Transform, Israel, *Journal Geodynamics* 24, 11-20.
- Marco, S., Rockwell, T.K., Heimann, A., Frieslander, U. & Agnon, A. 2005. Late Holocene Activity of the Dead Sea Transform Revealed in 3D Palaeoseismic Trenches on Jordan Gorge Segment, *Earth and Planetary Science Letters* 234, 189-205.
- Quennell, A.M. 1956. Tectonics of the Dead Sea Rift, in *Asociacion de Servicios Geologicos Africanos, Congreso Geologico International, 20th session, Mexico*, 385-405.
- Sadeh, M., Hamiel, Y., Ziv, A., Bock, Y., Fang, P. & Wdowinski, S. 2012. Crustal Deformation Along the Dead Sea Transform and the Carmel Fault Inferred from 12 Years of GPS Measurements, *J. Geophy. Res. Solid Earth* 117, B8, B08410.
- Sbeinati, M.R., Darawchah, R. & Mouty, M. 2005. The Historical Earthquakes of Syria: An Analysis of Large and Moderate Earthquakes from 1365 B.C to 1900 A.D., *Annals of Geophysics*, 48, 347 – 435.
- Wdowinski, S., Bock, Y., Baer, G., Prawirodirdjo, L., Bechor, N., Naaman, S., Knafo, R., Forrai, Y. & Melzer, Y. 2004. GPS Measurements of Current Crustal Movements Along the Dead Sea Fault, *Journal of Geophysical Research*, 109, B05403.